12

Magneto-rheological technology for human-machine interaction

Jose Lozada[1], Samuel Roselier[1], Florian Periquet\Xavier Boutillon[2] and Moustapha Hafez[1]
[1]*CEA-LIST, Sensory Interfaces Laboratory, 18 route du panorama, 92265 Fontenay-aux-Roses Cedex, France* [2]

1. Introduction

Human Machine Interfaces aim to give feedback to the user according to a given mechanical model or behavior. These systems are in constant interaction with the users senses. Haptic interfaces are mechatronic systems designed for providing force and tactile feedback to the operator while immersed into a virtual environment. The user inputs a motion or force into the system that reacts to this mechanical energy according to the virtual environment dynamical behavior.
The mechanical behavior needed to give correct feedback is then directly related to the mechanical impedance of human being. The system should be capable to display free motion as well as a rigid contact (for virtual reality applications). Traditional actuators, DC motors for example, are limited due to stability issues for high forces and usually their weight and size do not allow free motion.
Magneto-rheological fluids can be used to design semi-active systems (controlled damping or braking forces) that dissipate the mechanical energy applied by the user, this ensures their stability over all the working range. Moreover, the fluid exhibits a ~1 ms response time that permits real time control in the human interaction bandwidth.
Two basic operational modes have been reported for MR fluids: the "valve mode" and the "direct shear mode" Jolly et al. [1999]. Active dampers usually operate in the valve mode in order to develop high stiffness and damping. The potential drawback of systems based on this mode of operation is the high level of frictional forces induced by the piston configuration, even in the absence of magnetic field.
Current limitations for the magneto-rheological devices are often due to the design which is either in a brake configuration or a piston design. These limitations are mainly high uncontrolled forces due to friction and high inertia because of heavy moving parts. We propose in this work, a novel operating mode that reduces uncontrolled forces as well as the inertia of moving parts. This operating mode is based on shearing the fluid by a thin element (plate or cylinder), rather than shearing with the magnetic poles, increasing the performances and reducing the overall size.
We present the modeling and experimental characterization of the novel operating mode through two haptic interfaces.

The first example concerns the design of a haptic interface for musical keyboards. The presented system aim at reproducing the behavior of a traditional piano to give high quality feedback to a musician using a numerical keyboard. The system is then capable of precise force feedback controlled in real time for fast actuation.
The second illustrating example is a novel Human Machine Interface for automotive cockpits. The behavior of the system is given by prerecorded behaviors. The system should be user friendly, easy to use, stable and compact while generating moderate torque.
Both systems use the novel actuation principle, in a linear configuration for the first one and in a rotational configuration for the second.

2. Magneto-rheological (MR) Fluids Behaviour

"Rheological fluids" are liquids with viscosity properties that can be modified by an external stimulus. This stimulus can be a magnetic or electric field. In both cases, the external field acts on the micron sized particles in suspension into the carrier fluid. These particles form chains along the magnetic or electric flux lines thereby the apparent viscosity of the fluid increases as the external field intensity increases. The rheological modification can be exploited to dissipate the mechanical energy applied by the user. This semi-active behavior makes these fluids particularly interesting for real-time controlled systems because of their intrinsic stability.
We can cite two different technologies, magneto-rheological (MR) and electro-rheological (ER) fluids according to the external field nature. Their properties are similar but their integration on a controlled user friendly system is different. MR fluids use low voltage (~10V) and current up to 2A input whereas ER fluids use high voltage (~2kV) which limit the application, and low current (~10mA). The electrical power consumption is then more or less equivalent. Magnetic field generation needs coils and ferromagnetic parts which makes the MR-fluid-based systems more bulky than ER-based systems.
The resistant force available is a function of the yield stress under the maximum field intensity (given by saturation for magnetic field and by dielectric insulation for electric field). This maximum yield stress is of about 100 kPa for MR-fluids and 5 kPa for ER-fluids. The maximum resistant force is then 20 times higher for a MR-based system at equal active surface. The table 1.1 shows a comparison of typical values for both fluids.
Low voltage and higher yield stress make MR-fluids better for mass-market applications and for interfaces which are in direct contact with the operator.

2.1 Working Principle

Magneto-rheological fluids are suspensions of ferrous particles of a few microns size (typically 1 to 10 /xm) in a carrying fluid such as water or oil (synthetic or mineral oil). In the absence of a magnetic field, the fluid

Property	ER fluid	MR fluid
Yield strength (Field)	2–5 kPa (3–5 kV/mm) Field limited by breakdown	50–100 kPa (150–250 kA/m) Field limited by saturation
Viscosity (No field)	0.2–0.3 Pas at 25°C	0.2–0.3 Pas at 25°C
Operating temperature	+10–+90°C (ionic, DC) -25–+125°C (non-ionic, AC)	-40–+150°C (Limited by the carrier fluid)
Current density	2–15 mA/cm² (4kV/mm, 25°C) (x 10–100 at 90°C)	Can energise with permanent magnets
Specific gravity	1–2.5	3–4
Ancillary materials	Any (conductive surfaces)	Iron/steel
Colour	Any, opaque or transparent	Brown, black, grey/opaque

Table 1. Typical values for MR and ER fluids [Carlson et al., 1996]

behaves like a Newtonian[1] fluid. It's viscosity depends on that of the carrying fluid and on the concentration of particles.
Usually the particles represent 80 to 85% of the fluid weight which corresponds to 20 to 40 % of the volume if the carrying fluid is a mineral oil. MR-fluids can achieve shear stress of 100 kPa under a magnetic field of 200 kA/m.
In the presence of a magnetic field, the particles align themselves and form chains along the magnetic flux lines. These cohesive chains resist to the fluid flow. The amplitude of the magnetic field controls the apparent viscosity.
According to [LORD, Dec. 1999], the Bingham rheological model - Eq (1.1) - is used to describe the fluid behavior under direct shear.

$$\tau = \eta\dot{\gamma} + \tau_y(H)\hat{\dot{\gamma}} \tag{1}$$

where the operator $\hat{z}$ is defined by

$$\hat{z}\begin{cases} = Sign(z) & \text{for } |z| > 0 \\ \in [-1,1] & \text{for } z = 0 \end{cases} \tag{2}$$

In (1), τ is the shear stress, γ the shear strain, η the fluid viscosity, and τ_y a magnetic field dependent yield stress. Figure 1 shows the theoretical behavior of MR-fluids under direct

[1] A Newtonian fluid is characterized by a shear stress lineary dependent from the shear strain rate

shear. If the magnetic field is controlled as a function of the shear rate, we obtain a group of operating points. The apparent viscosity of the fluid can then be controlled.
The particles organization under a magnetic field follow five steps (see figure 2):
• when there is no magnetic field, the particles are distributed homogeneously in the carrier fluid
• a magnetic field produces a local magnetization of the ferrous particles
'A Newtonian fluid is characterized by a shear stress linearly dependent from the shear strain rate

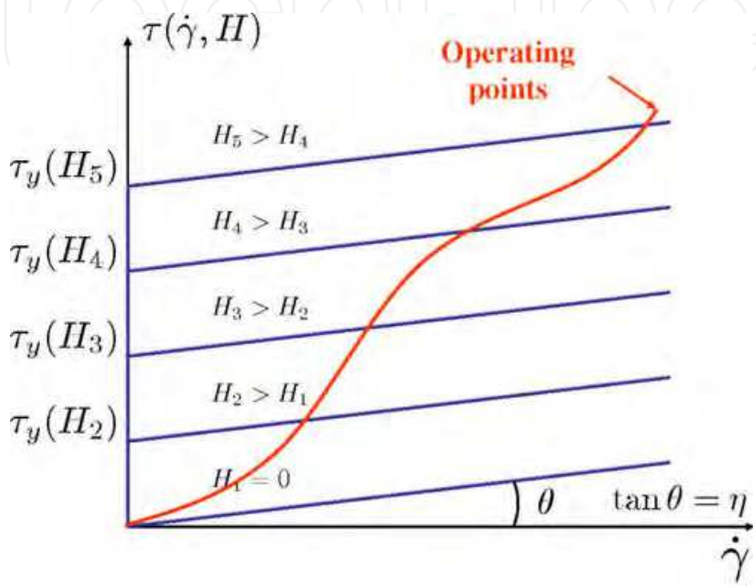

Fig. 1. Theoretical rheogram of a MR-fluid

• the ferrous particles act as magnetic dipoles that attract themselves
• under these attracting forces the particles form chains along the magnetic flux lines
• if the magnetic field is canceled, the thermal agitation brakes the chains and disperse the particles

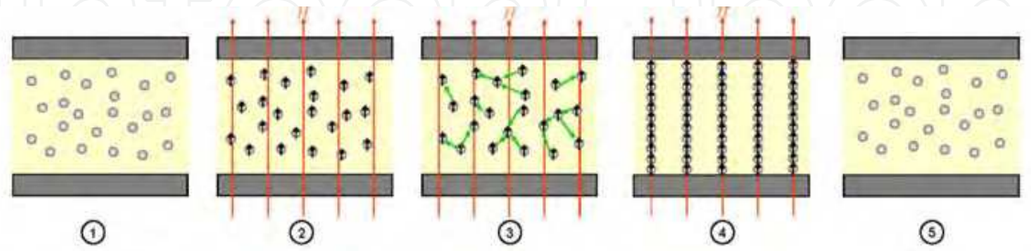

Fig. 2. Magneto-rheological effect

Since the magnetic field can only increase the apparent viscosity, systems based on MR fluids are intrinsically dissipative. The induced stability makes them appealing for usage in haptic interfaces.

2.2 Operating Modes

Two basic operational modes have been reported for MR fluids: the "valve mode" and the "direct shear mode" [Jolly et al., 1999]. Valve mode (see figure 3) is driven by a pressure drop between two cavities which creates a fluid flow pass an active zone. A magnetic field applied across the active zone increases the apparent viscosity of the fluid into the active zone thereby increasing the pressure difference.

Active dampers usually operate in the valve mode in order to develop high stiffness and damping. The potential drawback of systems based on this mode of operation is the high level of frictional forces induced by the piston configuration, even in the absence of magnetic field.

In the direct shear mode(see figure 4), the fluid is sheared by the relative motion between the magnetic poles, as in rotating machines such as brakes or clutches that do not need to produce large forces [Ahmadian,2002].

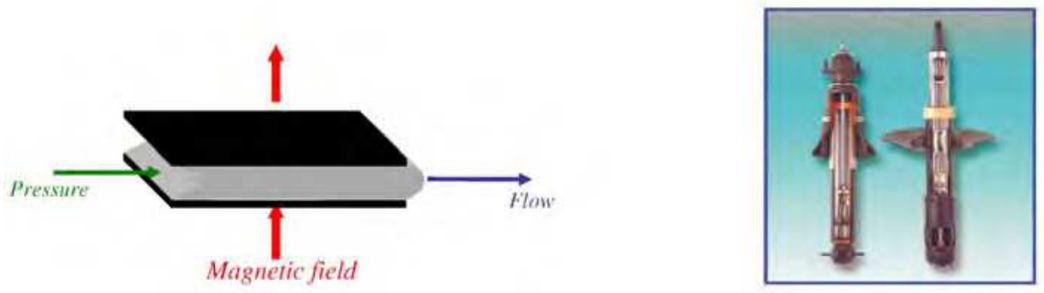

Fig. 3. Valve mode and application example: automotive damper [Delphi, 2005]

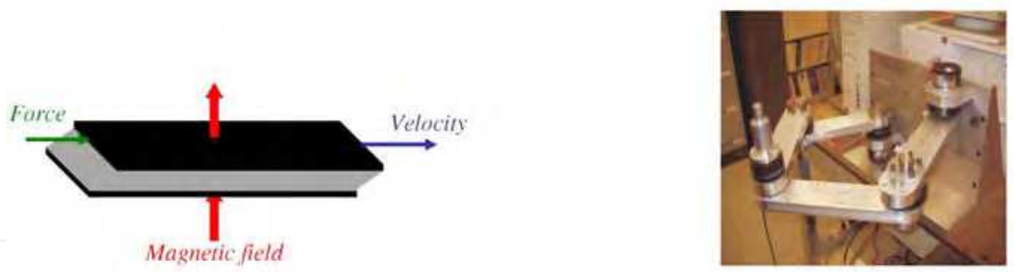

Fig. 4. Valve mode and application example: semi-active haptic interface [Reed and Book, 2004]

The relative motion of magnetic poles shears the particle chains which mechanical resistance is a function of the magnetic field, the shear stress increases as the magnetic field increases. In most cases, the rotor is

magnetic. However, the drawback of this operational mode is a large inertia of the moving parts. In order to lower the inertia, we introduce a novelty to the latter mode [Lozada et al., 2007]. Poles are held fixed and the gap between them is filled with MR fluid. A thin plate moving within the gap shears the fluid (see figure 5). This operating mode is used on both applications presented further. The haptic interface for musical keyboards uses it in a linear way and the MR-drive uses it in a rotational configuration (see figure 20).

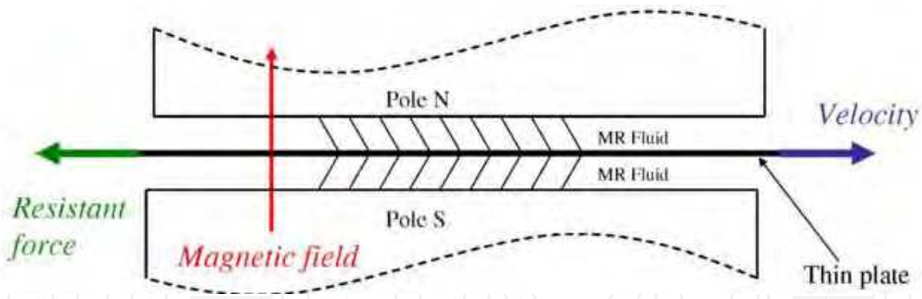

Fig. 5. Novel interaction principle: thin plate shear between the magnetic poles

2.3 Experimental Characterization and Modeling for the Novel Actuation Principle

The Bingham rheological model is not entirely satisfactory for the use of MR fluid in the context of the haptic interfaces presented further.

Usually in rotating machines under operating conditions, the relative velocity is usually high and the shear stress exceeds the yield stress: the behavior below the threshold can be neglected (see eq. (1)). In the application of a haptic interface, the velocity of the moving device of the interface changes continuously, the dynamics of the system is controlled in real-time by means of the control parameter H. Since a permanent regime is seldom reached, the behavior below the yield stress must be considered.

The function fluid behavior when sheared by a thin magnetic plate has been characterized by the experimental procedure described below. The device represented in Fig. 6 is composed of two magnetic poles (1), two coils (2), a plate support (3), a fluid container supporting also the poles and the coils (4), a frame (5), and a force/torque sensor (6).

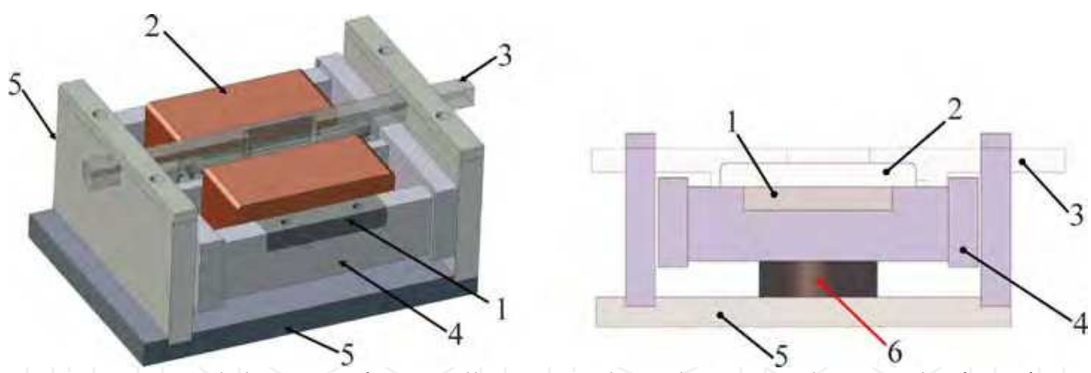

Fig. 6. Experimental device. Left: overall view; Right: side view indicating the force/torque sensor (6) position

The MR fluid fills the gap between the magnetic poles in which a 0.15 mm thick plate made of magnetic material moves linearly, shearing the fluid. Electrical current in coils induce a controlled magnetic field across the gap.

The plate support (Fig. 7.) is made of aluminum, two nuts, and two screws. The plate is attached to the nuts by metal pins. Screws control the tensile stress in the plate, thus ensuring flatness. This whole slider is constrained to move linearly by the frame (5).

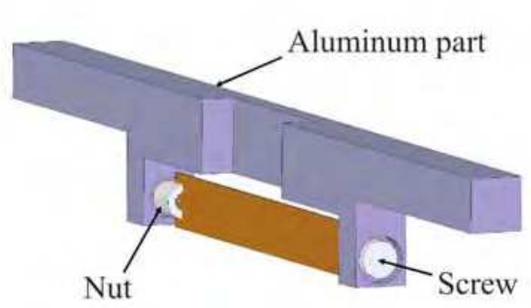

Fig. 7. Slider: plate and support

A test consists in applying an arbitrary motion $\xi(t)$ to the slider for a given current I in the coils.

The motion ξ of the slider is measured by a non-contact displacement sensor (Keyence, LB-72) and gives access to the shear strain. In order to measure the interaction forces between the slider and the MR fluid, the fluid container has been isolated mechanically from the frame and attached to a strain gauge 6-axis force sensor (ATI mini 40). This sensor (6) is placed between the fluid container (4) and the supporting frame (5) so that reaction forces and torques are fully transmitted to the supporting frame through the force/torque sensor (Fig. 6). The system guiding the slider is part of the frame which ensures that the corresponding friction is not applied to the force sensor. A careful calibration yields the relationships that transform the measurements of the sensor into the force F_s exerted by the slider on the MR fluid.

In this experiment, the fluid is sheared on each side of the plate, each facing a magnetic pole. The device has been designed so that the gaps and the shear areas associated to the north and the south pole are the same. It follows that the shear strain and shear stress are identical on each side of the plate. With the gap g = 0.5 mm, the area associated to each pole A = 400 mm^2, and £ the displacement of the plate.

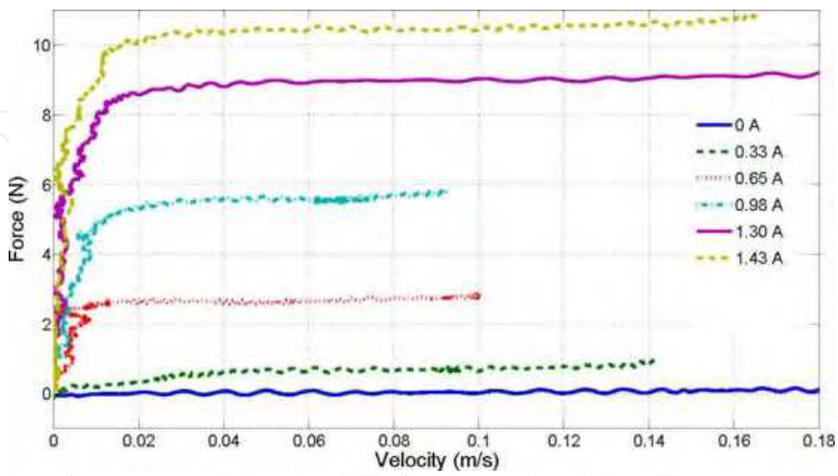

Fig. 8. Shearing force exerted by the MR fluid on the slider. The curves correspond to different levels of current in the coils, proportional to the the magnetic field.

The curves of figure 1.8 indicates two different regimes:

- the Bingham behavior is observed above a certain level of the force F_s with the same linear relationship between the increase in force and the increase in velocity, as described by (1),
- the transition regime where the force increases from 0 to the force threshold.

In the Bingham regime, the yield force increases with the magnetic field. Since the reluctance of the magnetic circuit is not altered by the motion of the slider, the magnetic field *H* is assumed to be proportional to the value *I* of the current. This relationship has not been quantitatively measured.
The Bingham regime is analyzed in Fig. 9. the parameters η and τ_y are obtained by fitting the experimental data points of the Bigham region (here: for a velocity above 0.0136 m/s) to the prediction of Eq. (1). The viscosity is found to be 2.8 Pa.s and the yield stress τ_y 12.4 kPa (force threshold 9.92 N).
When the applied shear stress τ is lower than the yield stress τ_y (H), we have observed that the behavior of the fluid depends also on the shear strain γ. We propose the following modified rheological model with three state-parameters γ, $\dot{\gamma}$, and H :

$$\tau = \eta\dot{\gamma} + \hat{\gamma}\min\{G(\gamma), \tau_y\} \tag{3}$$

where the value of τ_y and the function $G(\gamma)$ depend on the magnetic field H. Since, the carrying fluid is not expected to react significantly to a magnetic field, the viscosity η is assumed to be constant but depends on the particle content of the fluid.

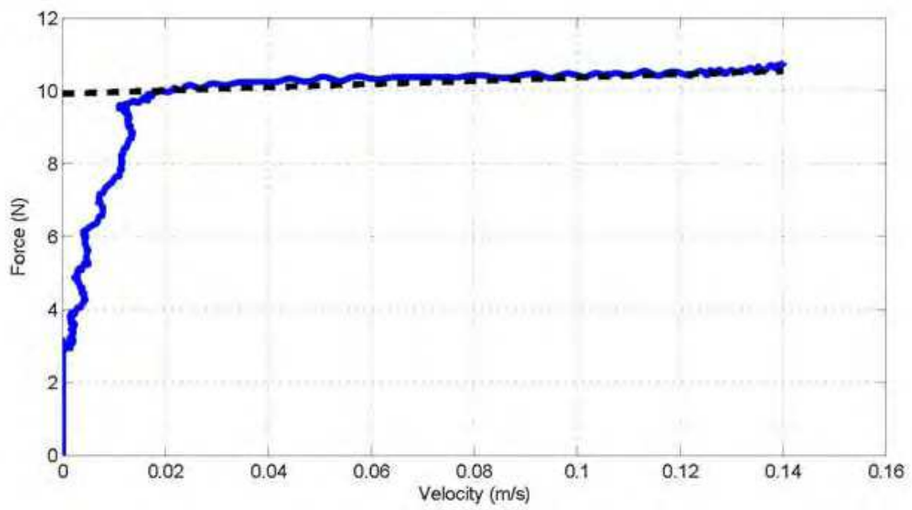

Fig. 9. Experimental results and predicted behavior according to the Bingham model of the MR fluid. Since one of the state variable of the fluid is not represented, the model is not valid in the transient region below the Bingham regime.

The local rheological model given by equation (3) is integrated as:

$$F_t = 2A\left|G\left(\frac{\xi}{g}\right)\right|$$
$$F_s = \eta\frac{2A}{g}\dot{\xi} + \hat{\xi}\min\{F_t, 2A\tau_y\} \quad (4)$$

Where F_t is the magnitude of the transition force between the fluid the slider.

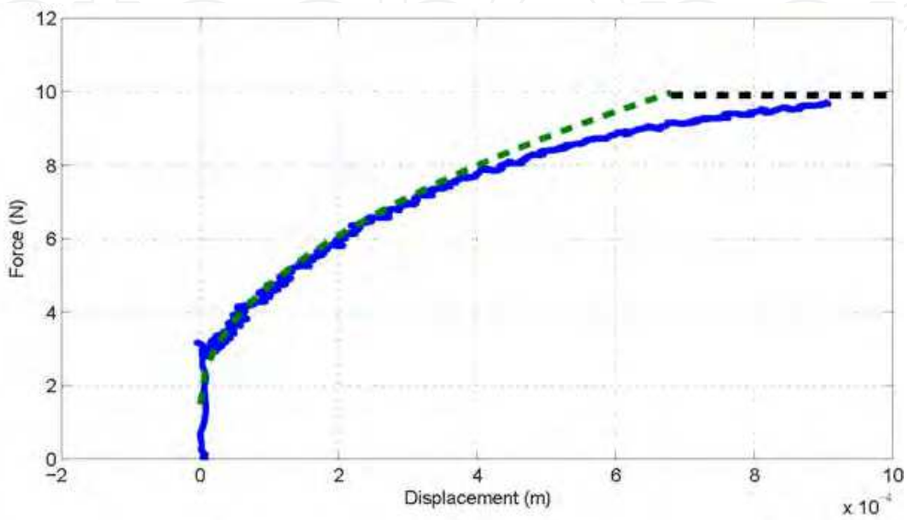

Fig. 10. Experimental results and fitted analytical model for the transient force F_t below the Bingham regime. The horizontal dashed line corresponds to the force threshold of the Bingham model.

The transition regime is analyzed in Fig. 10 the plotted force is F_t as a function of the displacement ξ of the plate. The force F_t is obtained by subtracting $2A\eta\dot{\xi}/g$ from the measurement of F_s with the numerical value of η given by the previous optimization. It appears that F_t is well fitted by the fllowing expression:

$$F_t = F_0 + \phi\sqrt{\xi} \quad (5)$$

with $F_0 = 1.5\text{N}$ and $\phi = 325\text{uSI}$. A log-log plot (not shown here) confirms the value $1/2$ of the exponent. One observes also a transition between the behavior described by Eq. 5 and the force threshold of the Bingham model. At this point, we have not found a physical ground for this analytical expression. We consider that the
mechanical behavior of the fluid is given by the expression:

$$\tau = \eta\dot{\gamma} + \hat{\dot{\gamma}}\min\{\tau_o + \varphi\sqrt{\gamma}, \tau_y\} \quad (6)$$

with $\tau_0 = 1.875\text{kPa}$ and $\varphi = 401\text{kPa}$.
Finally, the yield stress is a linear function of the magnetic field in a MR fluid until saturation occurs [LORD, 2005]. In the absence of physical understanding for the rheological behavior

below the Bingham threshold, we assume that the parameters τ_0 and φ also vary linearly with the magnetic field *H*:

$$\tau_y = K_y H \quad \tau_0 = K_0 H \quad \varphi = K_\varphi H \tag{7}$$

The proportionality constants are derived numerically from the results of the test described above and by a determination of *H* based on the analysis of the magnetic circuit.
The fluid behavior described above is used to simulate and control the haptic interfaces presented further. The experimental characterization gives also a way to precisely estimate the maximum resistant forces given by the interfaces according to its design.

3. Haptic Interface for Musical Keyboards

The traditional acoustic piano action mechanism (Fig. 11.) is composed of many different parts of wood, wool felt, leather, metal, and steel-springs. These parts form a multi-degree-of-freedom system that transmits energy from the player to the hammer. In return, the action mechanism generates a specific tactile rendering that is felt by pianists during playing. The haptic feedback is essential for a precise control of timing and loudness [Repp, 1999].

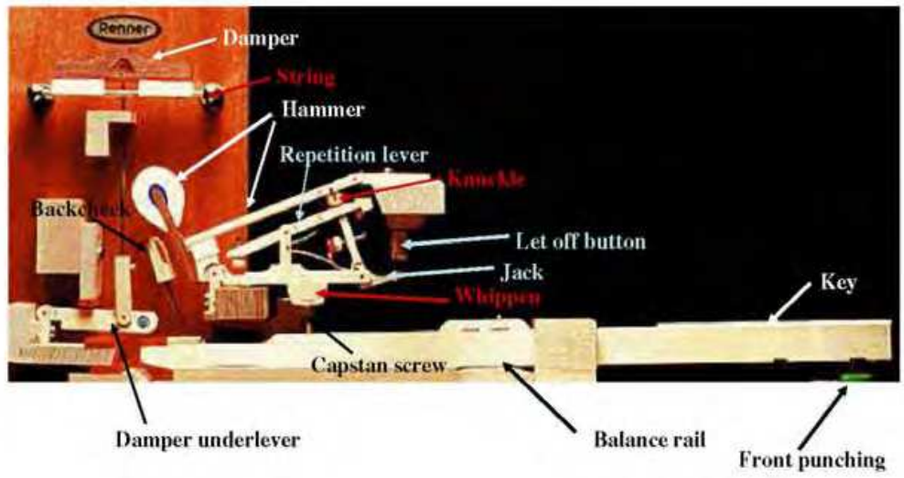

Fig. 11. Traditional piano action mechanism

The action mechanisms used in numerical pianos are much simpler but provide a poor haptic feedback. In the last few years, many developments have been carried out by keyboard manufacturers in order to improve the touch feeling of their products. Most of these systems are not actively controlled and are based on simplified models of the dynamical behavior of traditional pianos. According to users, improvements are still required in terms of size, performance and realism of the device.
Active systems capable of reproducing the traditional piano dynamics have been addressed by [Gillespie, 1996] [Cadoz et al., 1990] and commercial products [Meisel, Nov. 2003]. They are based on simplified models or pre-recorded dynamics that do not satisfactorily match the

dynamical behavior of the traditional piano key. Moreover, the size of these systems based on electromagnetic actuators is not suitable for an industrial keyboard implementation.
The resistant force provided by the traditional piano action mechanism varies from 0.5 N (the minimum force that initiates key motion), to 15N (at *fortissimo* nuance, according to [D. Parlitz, 1998]). Extensive measurements of the kinematics of a grand piano action mechanism [Askenfelt and Jansson, 1990] [Askenfelt and Jansson, 1991] indicate that the duration of the key motion varies from 20 to 250 ms depending on the nuance whereas the key velocity varies from 0.1 $m.s^{-1}$ to 0.6 $m.s^{-1}$.
We present here a system aimed at reproducing the dynamical behavior of the piano action. The traditional mechanism is passive and it can generate a opposite force to the finger's motion during the whole duration of the note stroke. Therefore, we have chosen to develop a system controlling a *resistant* force in real-time, dissipating the mechanical energy given by the pianist by means of a magneto-rheological fluid, sheared by a slider pushed by a simple lever.

3.1 Interface Description

The haptic piano interface shown in Fig. 12. is composed of two main parts: a mechanical structure with various sensors (not shown in figure) and an active system composed of a slider and electromagnetic elements with MR fluid, similar to those described in the previous section.

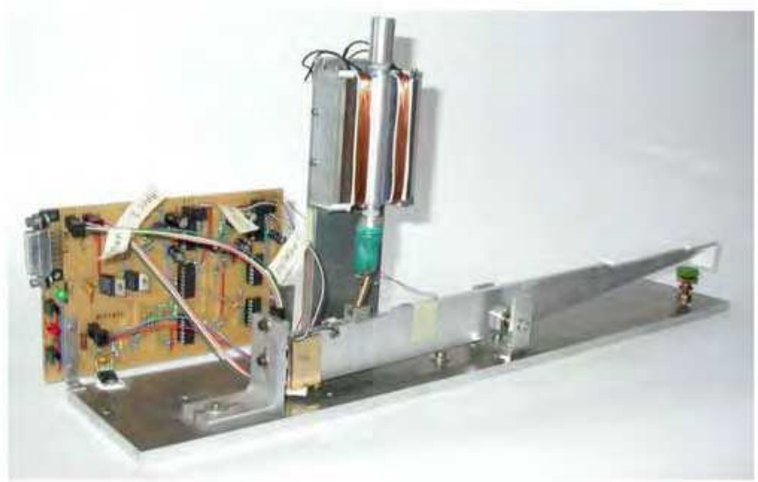

Fig. 12. Piano Interface with Active Feedback

In this prototype, the aluminum key has the same inertia and the same geometry as those of a traditional wooden white key. The pivot between the key and the keybed is ensured by high quality bearings. The contact between the front-end of the key and the keybed is ensured by the same felt pad as in traditional pianos.
A connecting rod is pinned between the key and the slider of the active system in order to transform the rotational motion of the key into a translational motion for the slider.
The motion of the key is measured by *MEMS* accelerometers (ADXL 103 and ADXL 321 for two different measurement ranges 0... 10 $m.s^{-2}$ and 0... 150 $m.s^{-2}$); this instrumentation would be sufficient for the interface operational usage.

The active system (Fig. 13.) is composed a magnetic circuit (1), moving-parts (2), sealing fixtures (3) encapsulating the MR fluid, and guiding parts (4). The whole system is attached to a fixed frame (5).

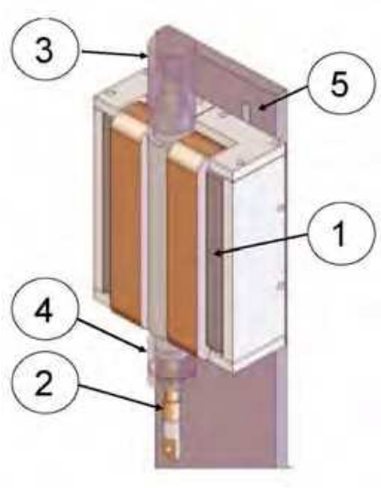

Fig.13. View of the active system

The magnetic circuit (Fig. 14.) includes two I "-shape ferromagnetic cores, each of them supporting a 100-turn coil. This circuit is closed by the 1 mm gap containing the MR fluid. The magnetic field across the gap activates the MR fluid. The moving part consists of a slider formed by three brass rods and a 0.15 mm thick iron plate (left part of Fig. 14.).
The slider moves inside the gap between the poles filled by the MR fluid. A central part with a slot (right part of Fig. 14.) is positioned around the poles so that the magnetic poles face each other across the slot. This part seals the vertical openings of the gap. The top and bottom of the gap are sealed by a solid cap on top ((3) in Fig. 13.), a tube attached to the bottom of the central part, and a nitrile membrane glued to this tube. The two bottom rods of the slider are screwed together through a hole at the center of the membrane as to pinch it and ensure proofness. This design is an alternative to the usual O-ring joint arrangement which generates more friction.

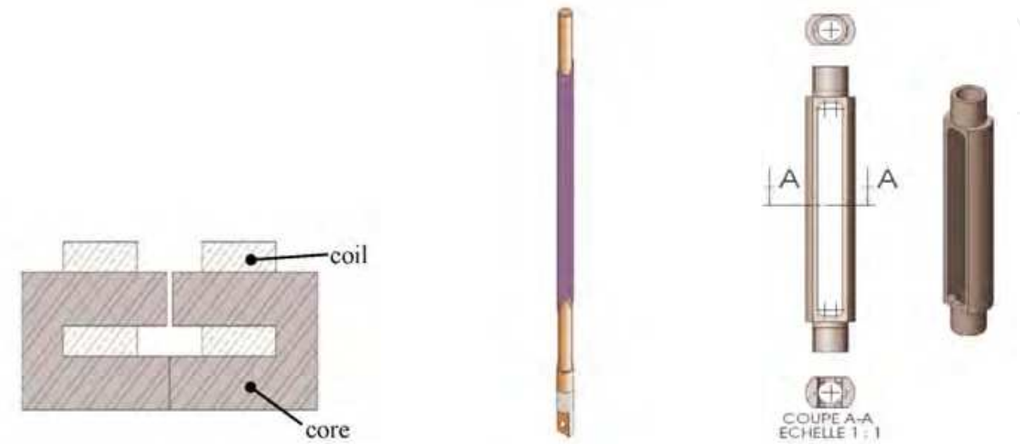

Fig. 14. Cross-section view of the magnetic circuit (left), Slider (center) and slot frame (right)

A guiding mechanism, enclosed in the tube attached to the bottom of the central part, is required to maintain the lateral position of the slider at the center of the gap and to avoid contacts between the plate and the poles.
With a current of 1 A in the coils, this active system can produce a force of 50 N opposing the motion, nearly independent of the velocity. This force becomes 25 N at the key front end, much higher than the 15 N required by specifications . A further optimization could help reducing size and power consumption.

3.2 Mechatronic Model of the Interface

The behavior of the haptic keyboard interface results from mechanical, magnetic, and electrical interactions. Since they are independent up to a certain extent, they are presented separately here: mechanical modeling, electromagnetic behavior, and coupling due to the MR fluid; finally, a box-diagram presents synthetically how the whole system operates and how its behavior can be computed.

Mechanical modeling

The mechanical model of the interface is based on the following approximations:
- all parts are rigid bodies
- friction is negligible in rotational links
- the mass and the inertia of the connecting rod are negligible
- the angle θ describing the motion of the key remains very small: $\cos\theta \approx 1, \sin\theta \approx \theta$.

A schematic view of the interface is presented in Fig. 15. The points of interest for the model are represented either those subjected to a particular force or centers of rotation, as summarized in Table 2.

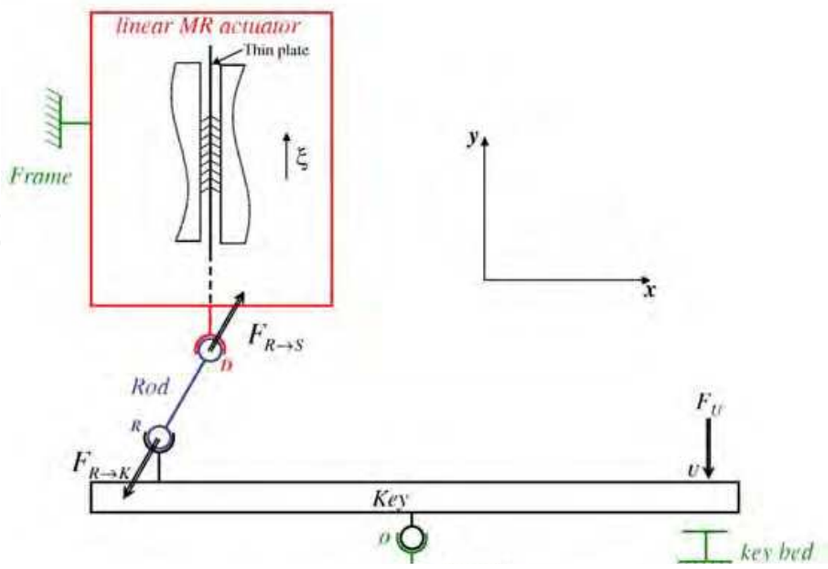

Fig. 15. Shematic representaion of the interface. Some forces are represented.

Point	x	y	Forces	Description
U	x_U	y_U	$\overrightarrow{F_U}$	Force applied by the user (musician)
T	x_T	y_T	$\overrightarrow{F_T}$	Front end keybed contact
G	x_G	y_G	$m_K\,\overrightarrow{g}$	Key weight
R	x_R	$y_R \approx y_{R_0} + x_R\theta$	$\overrightarrow{F_{R\to K}}$	Force exerted by the rod on the key
D	x_D	$y_D = \xi$	$\overrightarrow{F_{S\to R}}$	Force exerted by the slider on the rod
			$F_{g,y}\,\overrightarrow{y}$	Friction exerted by the guiding system

Table 2. Geometrical parameters and associated dynamical variables

Thee coordinates listed in the second and third columns of Table 2 belong to the reference frame $(O, \overrightarrow{x}, \overrightarrow{y})$. The axis $\overrightarrow{Ox}$ corresponds to the horizontal.
It is now described how constraints on the three solid bodies - key, rod, and slider - reduce the number of mechanical degrees of freedom of the system to one. The key is constrained to rotate with an angle θ around O. The motion of the slider is constrained to be a translation in the y directorion by ξ. In other words, the abscissa x_D of the top of the rod or bottom of the slider is kept constant. Let us define x_R as the abscissa of the bottom of the rod; since this point is attached to the key, x_R is also constant within the approximation given by $\cos\theta = 1$. The projection of the rod on Ox is therefore the constant L_x. Finally, the fixed 1ength L of the rod gives ξ as a function of θ:

$$\begin{aligned} & (y_D - y_R)^2 + (x_D - x_R)^2 = L^2 \\ \Rightarrow \quad & \xi^2 - 2y_{R_0}\xi + 2x_R y_{R_0}\theta(1-\xi) + y_{R_0}^2 + L_x^2 - L^2 = 0 \end{aligned} \tag{8}$$

to the first order in θ, with intuitive notations.
In normal use, the key is subjected to forces applied by the rod $\overrightarrow{F_{R\to K'}}$ the user $\overrightarrow{F_U}$, the contact with the key-bed at the front $\overrightarrow{F_T}$, and to its own weight. To zero-order in θ, the angular momentum balance yields:

$$\begin{aligned} J_K\ddot{\theta}\overrightarrow{z} \quad &= \quad m_K\overrightarrow{OG}\times\overrightarrow{g} + \overrightarrow{OR}\times\overrightarrow{F_{R\to K}} \\ & \quad +\overrightarrow{OU}\times\overrightarrow{F_U} + \overrightarrow{OT}\times\overrightarrow{F_T} \\ \Rightarrow \quad F_U x_U \quad & J_K\ddot{\theta} + m_K g x_G - F_T x_T - x_R F_{R\to K,y} \end{aligned} \tag{9}$$

where J_K is inertia momentum of the key in O, and m_K its mass.
In Eq. (9), the first term is derived from the measurement of $\ddot{\theta}$, the second term is constant, the force F_T exerted by the keybed at the end of the key motion depends on the

characteristics of the felt (not studied in this paper), and the last term is given by the following analysis.
Since the mass of the rod is neglected, forces on the rod are balanced:

$$F_{R\to K,x} = -F_{R\to S,x} \tag{10}$$
$$F_{R\to K,y} = -F_{R\to S,y} \tag{11}$$

The moments of forces are also balanced and may be derived at any point, for example in D:

$$F_{R\to K,y} = F_{R\to K,x}\tan\theta_R \tag{12}$$

where θ_R is a geometrical data given by $\cos\theta_R = \frac{L_x}{L}$
Coupling between the rod and the slider involves some friction due to the guiding system. It is assumed that friction is localized in D and follows the Coulomb model. With the geometrical setting represented in Fig. 15., the force $F_{g,y}$ exerted by the guiding system on the slider in the y direction is derived as follows:

$$F_{g,y} = -\mu F_{R\to S_x}\widehat{\dot{\xi}} \tag{13}$$
$$\text{Eq.}(10) \Rightarrow \quad F_{g,y} = +\mu F_{R\to K,x}\widehat{\dot{\xi}} \tag{14}$$
$$\text{Eq.}(12) \Rightarrow \quad F_{g,y} = \frac{\mu}{\tan\theta_R}F_{R\to K,y}\widehat{\dot{\xi}} \tag{15}$$

where μ is the friction coefficient of the guiding system.
Forces acting on the slider in its direction of motion are:
- the slider weight
- the friction force due to the guiding system $F_{g,y}$,
- the restoring force due to air compression in the fluid cavity, $F_{sp} = -k\xi + F_{sp0}$ where k is the stiffness of the spring equivalent to the compression of air in the cavity,
- the force applied by the rod, equal to $-F_{R\to K,y}$ according to the dynamics of the rod,
- the force F_f exerted by the MR fluid which can be calculated with (6).

Applying Newton's law to the slider yields:

$$m_S\ddot{\xi} = -m_s g + F_{g,y} + F_{sp} + F_{R\to S_y} + F_f \tag{16}$$

Finally:

$$F_{R\to K,y}\left(1 - \frac{\mu}{\tan\theta_R}\widehat{\dot{\xi}}\right) = -m_S\ddot{\xi} - m_s g - k\xi + F_{sp0} - \frac{\eta A_S}{g_f}\dot{\xi} - \widehat{\dot{\xi}}A_S\min\tau_0 + \varphi\sqrt{\frac{\xi}{g_f}}, y \tag{17}$$

where m_s is the mass of the slider, A_S the area of sheared flu id, and g_S the width of sheared fluid.

Electromagnetic modeling

The electromagnetic behavior of the coils and the magnetic circuit determines the magnetic field *H* in the MR fluid as a function of the voltage *V* applied to the coils.
Electrically, the system behaves as a *RL* circuit with:

$$L = \frac{N^2}{\mathcal{R}} \tag{18}$$

$$R_\rho \frac{4L_w}{\pi d_w^2} \tag{19}$$

where N is the number of turns, $\mathcal{R}$ is the reluctance of the magnetic circuit, ρ, L_w, and d_w are respectively the resistivity, the length, and the diameter of the wire.

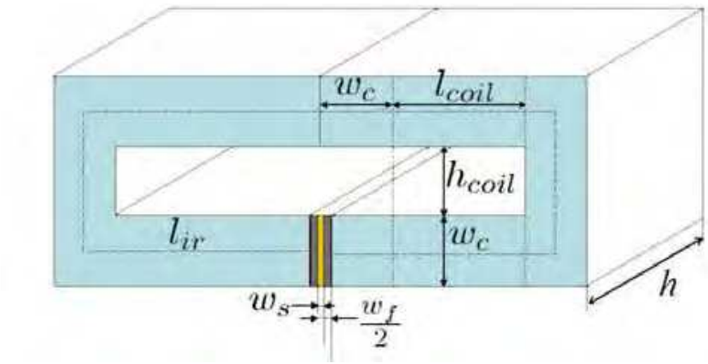

Fig. 16. Geometrical parameters for the magnetic circuit

The electrical equation of the system is (20):

$$L\frac{dI}{dt} + RI = V \tag{20}$$

A cross-section of the magnetic circuit is shown in Fig. 16. Its reluctance is:

$$\mathcal{R} = \mathcal{R}_s + \frac{g_f}{\mu_f A_f} \tag{21}$$

where $\mathcal{R}_s$ is the reluctance of the solid part of the magnetic circuit (ineluding the slider), g_f and A_f the total width and area of the fluid gap, and μ_f the permeability of the MR fluid. With μ_i and μ_p the magnetic permeabilities of the iron (used in the magnetic circuit) and the moving plate, l_i and e_i the average lengths of the magnetic lines in the iron magnetic circuit and in the slider, and A_i and A_p the cross section areas, the reluctance $\mathcal{R}_s$ is given by:

$$\mathcal{R}_s = \frac{l_i}{\mu_i A_i} + \frac{e_p}{\mu_p A_p} \tag{22}$$

The magneto-rheological effect in the fluid changes somewhat the permeability of the fluid; if this effect remains small, the total reluctance of the circuit can be considered constant and independent of the mechanical evolutions of the system: the magnetic flux is solely determined by the tension applied to the coils.
The Ampere's theorem yields (1.23):

$$NI = \mathcal{R}\Phi \tag{23}$$

where Φ is the magnetic flux in the circuit. Considering that the magnetic induction $\vec{B}$ is constant across the gap between the poles, the flux, the magnetic field H in the MR fluid is given by:

$$H = \frac{\Phi}{A_f \mu_f} \tag{24}$$

$$= \frac{NI}{\mathcal{R} A_f \mu_f} \tag{25}$$

In order to maximize the magnetic field, $\mathcal{R}$ must be kept as small as possible. This implies compactness of the circuit and a minimal width of the fluid gap (that improves also the validity of the approximation stated above). The former is limited by the size of the coils and the latter by mechanical constrains: rigidity of the slider plate and tolerance for smooth motion.

Block diagram of the haptic interface
All the models developed in the previous sections can be summarized biny the block-diagram of Fig. 1.17 which shows how the output force F_U felt ba the user is determined by the applied voltage V on the coils and by the angular motion θ.

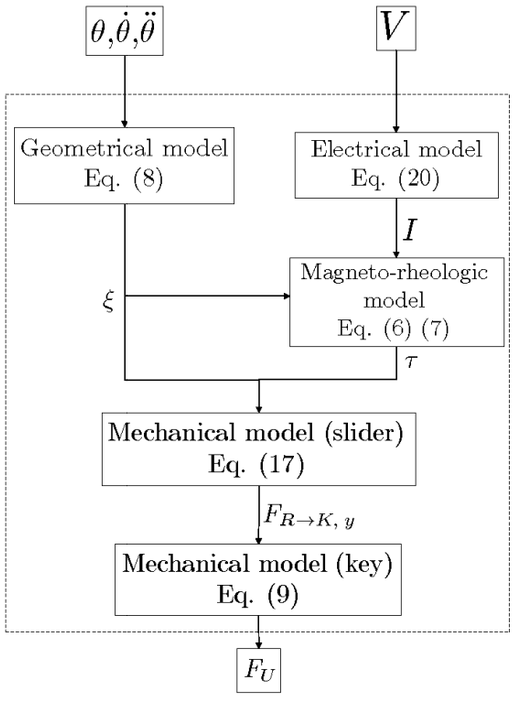

Fig. 17. Haptic piano interface model

At this point, it should be noticed that the user does not *impose* a force or a motion to the interface but follows its own {force-motion} law; consequenty, the choice of θ and F_U as input and output variables respectively is rather arbitrary. It has been guided by the availability, price, and ease of use of motion sensors rather than force sensors.
The system presented in this section exhibits all the required properties for displaying the behavior of a traditional piano, especially the force range $(0.5\mathrm{N}...50\mathrm{N})$ and the electrical response time (0.6 ms) The interface model presented above can be used for parameter identification and for the control strategy. Future work will implement a model-based real time control strategy that permits to link the interface to the dynamical model of a virtual piano. The virtual piano will give the needed force in real time and the control strategy should ensure that the force felt by the user corresponds to the desired force.
This interface is a linear application of the novel operating mode presented in section 1.2. The system performances are increased in regard to systems described on the literature of linear MR-actuators. The force ratio (controllable over passive forces) is of about 100. By applying this operating mode to a rotational interface, we can observe the same kind of advantages over existing systems as shown in section 1.4.

4. MR-Drive: A new 1-DOF MR Fluid Based Haptic Interface

GPS navigation, communication, climate and audio systems are widespread functions available in recent cars. The resulting control panels of such systems usually look like an array of controls. Moreover, some "all-in-one" button-based solutions have been developed and despite their ease of use, visual feedback is still necessary to activate the functions, even while driving [BMW, AUDI]. These developments have underlined the interest for haptics in cars. When using a force feedback button, different haptic patterns assigned to specific functions or areas within the menus of the HMI (Human Machine Interface) of be displayed. Haptic interaction decreases the visual load of the driver. Several button designs based on new actuation technologies are presented in [Melli-Huber et al., March 2003] and [Badescu et al., March 2002].

4.1 System design

The MR-Drive system (see figure 1.18) is composed of two magnetic poles facing each other (1), a coil around the central pole (2), a rare earth permanent magnet (3), all these parts are fixed to a frame (5). This architecture is defined as a permanent-electromagnet system. A thin cylinder (4) and a cap (6) are connected to the shaft (8) and guided by two bearings. A nitrile joint is used to prevent fluid leakage. The rotation angle is measured by an optical encoder (7). The thin cylinder rotates in the gap between the magnetic poles. This gap is filled with MR fluid.

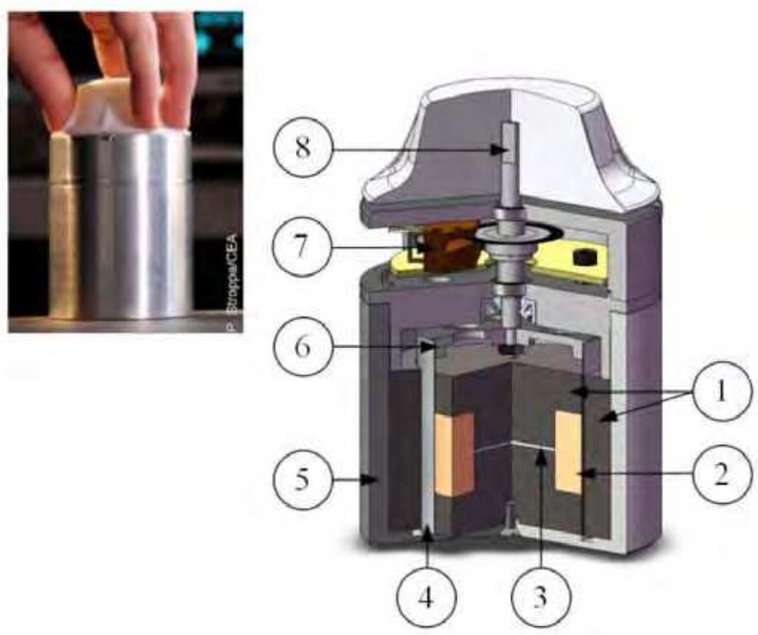

Fig. 18. Overall view of MR-drive

Figure 19 shows the different parts of the magnetic circuit. The thickness of the cylinder (center of figure 1.19) is 0.2 mm with an average diameter d_c of 44 mm. The height h of the magnetic circuit is 40 mm. The coil has an inner diameter of 27 mm and a thickness of 29 mm with 770 turns, its resistance is 24 ohms. Central and outer poles are made of pure iron Armco Telar 57 and the cylinder is made of conventional magnetic steel.

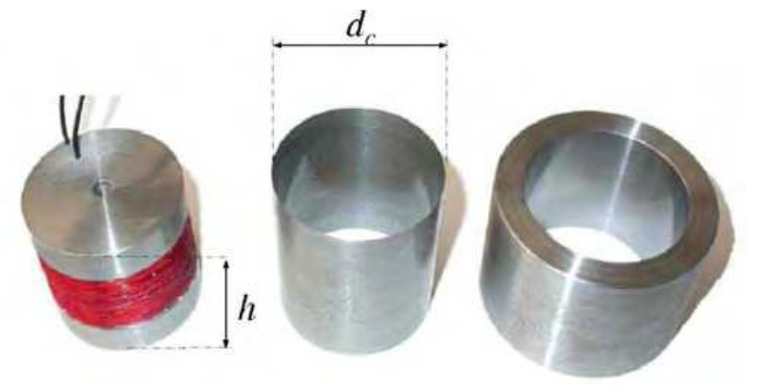

Fig. 19. Parts of the magnetic circuit. Coil arround the central pole (left), moving cilynder (center) and external pole (right)

Figure 20 shows the working principle of the MR-drive system. The shaft, that rotates when the system is actuated by the user, is linked to the cylinder. The cylinder rotates in the gap g between the two poles. The gap is 1 mm thick and it is filled with 4.5 cm^3 of MR fluid. The cylinder rotation shears the fluid into the gap which produces a resistant force tangent to the cylinder surface.

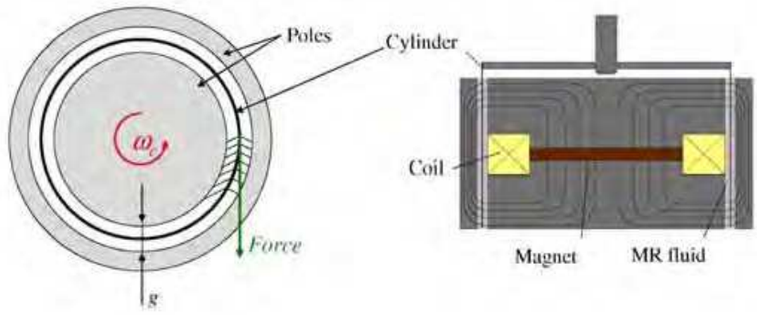

Fig. 20. Working principle

The operating mode of the system is a variation of the thin plate shear mode presented in section 1.2. When the user turns the button, the cylinder rotates around its axis and shears the MR fluid into the gap, the magnetic poles remain static. Thereby the inertia of the moving parts is highly reduced. A current applied to the coil generates a magnetic field across the gap. The value and the current direction set in the coil can either cancel or reinforce the magnetic field established by the magnet. Both the inner and outer surfaces of the thin cylinder shear the MR fluid, therefore the active surface is larger which increases the maximum torque.

4.2 Magnetic Simulation and Torque Estimation

The fluid is sheared at a small rate by a thin cylinder. The MR fluid model presented in section 1.2 can be applied to describe this device operation.
Lets dS be an elementary area of the cylinder defined by dS = dz x d0 where z is the vertical coordinate of the cylinder and 0 the circular coordinate. The magnetic circuit produces a magnetic field H assumed perpendicular to the surface dS. Under these conditions, the elementary torque is expressed as follows:

$$\frac{dT_z}{dS} = \frac{d_c}{2}\tau_y(H)dS \tag{26}$$

with d_c the inner diameter of the cylinder.
According to the model presented in 1.2.3, the yield stress τy is considered as a linear function of the magnetic field *H*. The magnetic circuit was designed to maintain the magnetic induction B under the fluid saturation which validates the linear approximation for the relationship between the magnetic field and the magnetic flux density. We define the two constants K_y and μ_f as follows:

$$\tau_y = K_y H \quad \text{and} \quad H = \tfrac{1}{\mu_f} B \tag{27}$$

The normal magnetic flux density B_s varies continuously along the two sides of the surface of the cylinder and it is a function of the vertical coordinate z. h is the height of the

magnetic circuit and the thickness e of the cylinder is neglected. The field dependent torque T_z is given by:

$$T_z = \iint_S \frac{d_c}{2} \frac{K_y}{\mu_f} |B_s(z)| \, dS \tag{28}$$

$$T_z = \frac{d_c}{2} \frac{K_y}{\mu_f} \int_0^{2\pi} \frac{d_c}{2} d\theta \int_0^h |B_s(z)| \, dz \tag{29}$$

$$T_z = \frac{d_c^2 \pi}{2} \frac{K_y}{\mu_f} \int_0^h |B_s(z)| \, dz \tag{30}$$

Simulations are carried out with FEMM[2] software . The positive values of the current through the coil reinforce the magnetic field of the magnet whereas the negative ones cancel it. The normal magnetic flux density has been simulated for currents in the coil ranging from -1.2 A to 2 A. The permanent magnet placed in the central pole is 1.6 mm height and has a diameter of 25.4 mm.

Figure 21-left presents the results of the simulation by Finite Elements Method of the magnetic circuit behavior with a current of 1.75 A in the coil. $|B|$ and the flux lines are represented. The central part of the magnetic circuit is near the saturation limit ; the value of $|B|$ is over 2 T. Normal flux density B_s along the gap between the central pole and the thin cylinder is extracted from this simulation. Figure 1.21-right presents its topology at different current levels. The minimum of $|B_s|$ (5 mT) is obtained with a current of -0.44 A. At 0 A, the value of $|B_s|$ is 0.3 T due to the presence of the magnet.

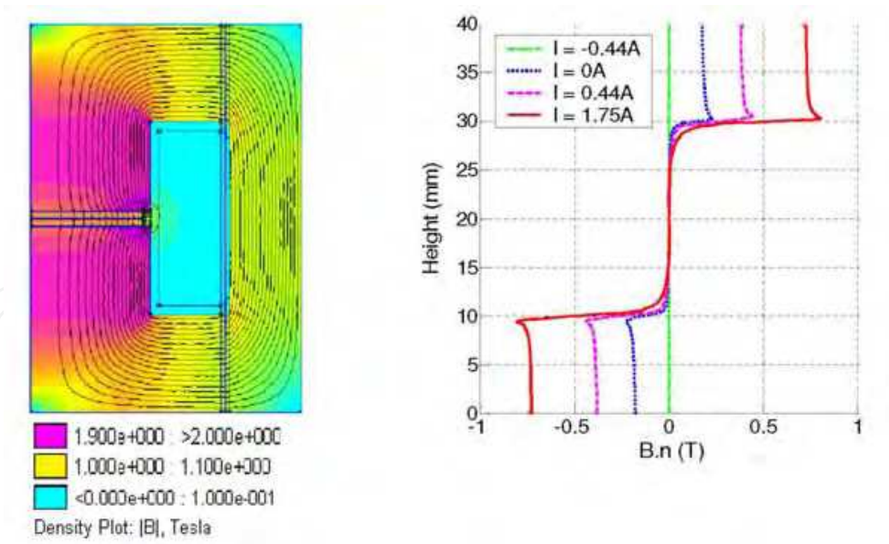

Fig. 21. Finite elements simulation of the magnetic field for a current of 1.75 A. Magnetic circuit (left) and normal magnetic flux density in the gap (right)

[2] http://femmfoster-miller.net

According to Eq. (30), the magnetic field density B_s has been integrated over the surface of the cylinder to simulate the maximum torque available. Results are reported in figure 22.

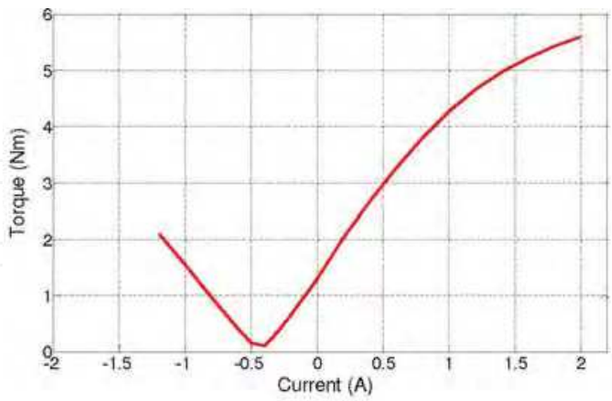

Fig. 22. Maximum torque estimation as a function of the current set in the coil

The minimum torque is obtained for a current of -0.44 A. The torque due to the presence of the magnet alone is 1.25 Nm and the maximum torque is expected over 5 Nm. Magnetic saturation of the material occurs for currents up to 1 A. Under -0.44 A, the magnetic field is inverted and the torque increases.

4.3 Experimental Results

An experimental setup (Figure 23) has been mounted to validate the simulations. A torque is applied to the shaft of the interface. The frame is mounted on a 6-degree of freedom force/torque sensor ATI mini40. The angular displacement of the shaft is measured with an optical encoder HEDS 5500. Data are recorded with Lab View software.

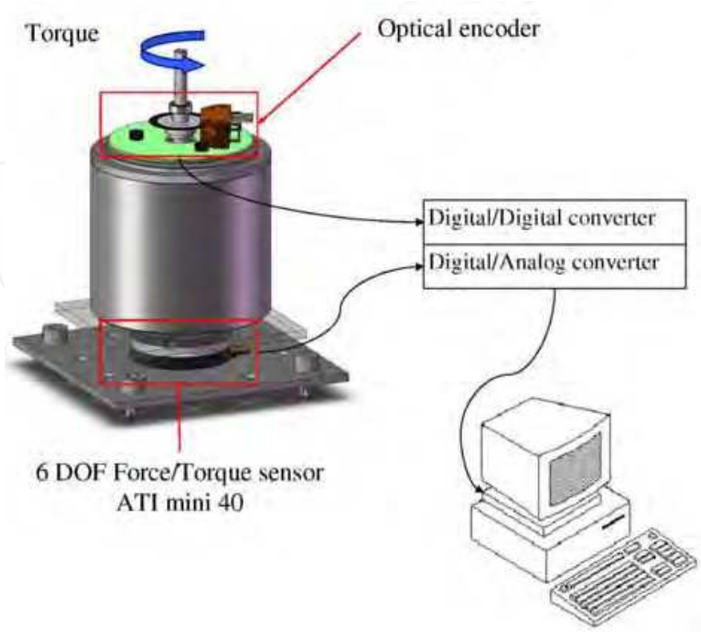

Fig. 23. Experimetal septup

Measurements have been carried out with current intensities through the coil between -1 A and 1.75 A. Results are reported in figure 1.24 and compared to the simulation.

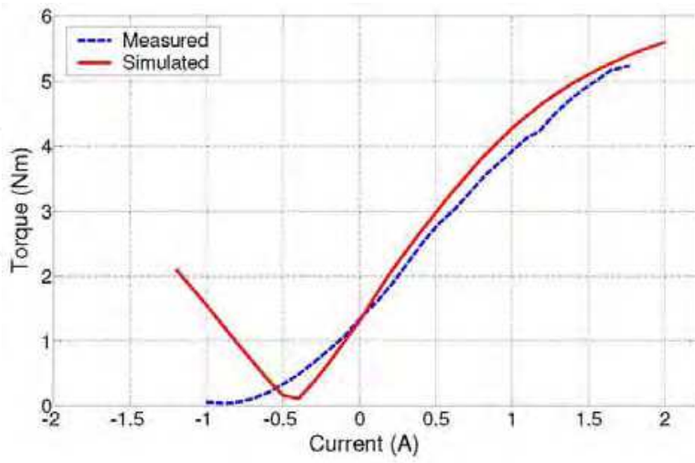

Fig. 24. Experimental results and comparison with numerical simulation

Experimental results and simulation are close for positive values of the current. The maximum deviation does not exceed 8%. Discrepancies can be observed for negative values of the current. The current intensity required to reach the minimum torque is -0.8 A which is twice more than the results of the simulations. This deviation is probably due to high values of the magnetic flux density at the surface of the magnet that might not be supported by the electromagnetic simulation. Simulating the non linear behavior of materials at high magnetic field densities should explicitly be mentioned [LORD, 2002].
It is worth noting that the minimum $T_{(min)}$ and the maximum $T_{(max)}$ torques measured are respectively 0.03Nm and 5.25Nm. The ratio between T_{max} and T_{min} is 175.

5. Conclusion and future work

Magneto-rheological fluids exhibit an apparent viscosity that varies as a function of an external magnetic field. This property can be exploited to the dissipate mechanical energy applied by the operator. Thereby, MR fluids based systems have a semi-active behavior which makes them intrinsically stable. Moreover, their low response time make them appealing for human machine interaction. Current limitations concern mainly the moving parts inertia or friction needed for proofness.
In order to reduce these limitations, a novel operating mode for magneto-rheological based systems is presented. This operating mode is based in shearing the MR fluid with a thin element (plate or cylinder). The thin element permits low inertia moving parts to increase the mechanical bandwidth while increasing the active surface thereby increasing the maximum force.
Two application design using this novel approach are presented. The piano haptic interface which uses the operating mode in a linear configuration. The design allows high force range and quick response time needed to reproduce the traditional piano dynamical behavior. A novel haptic interface for musical keyboards has been presented in this paper, based on controlled damping by a magneto-rheological fluid in its direct shear mode:

• the standard shear mode principle with relative motion between poles was replaced by a slider (made of a thin plate) moving between the static poles in order to reduce overall size and to allow the implementation on a real keyboard,
• the fluid behavior in this shear mode was explored experimentally and a new model has been derived for the behavior of the fluid below the Bingham threshold.

The analytical predictive model of the overall system was presented and implemented. The parameters influence on the global behavior has been studied and the critical parameters have been identified.

Future work will address the physical nature of the rheological model below the Bingham threshold, the improvement of the measurement of the key motion in order to improve the accuracy of the predicted behavior of the interface. A real-time control scheme will be implemented. In order to avoid the use of a force sensor on each key, we will explore an open loop control approach, using a traditional piano dynamical model and the interface model.

The Mr-drive system is a HMI for automotive applications. It exhibits high torque/volume ratio in comparison with traditional actuators and intrinsic stability. The design of a rotary interface based on magneto-rheological fluids has been presented. A thin cylinder that shears the fluid in a gap between two static poles minimizes the overall inertia. In addition, a permanent-electromagnet has been introduced to widen the output torque range. The ratio between the minimum and the maximum torque is 175. This ratio is far better than all what has been reported so far in the literature on MR brakes. Finite Element simulation and experimental measurements have been compared. The first results are promising and the application of the actuation principle to other haptic applications will be studied.

6. References

M. Ahmadian. On the application of magneto-rheological fluid technology for improving rail vehicle dynamics. In *International Mechanical Engineers Conference.* New Orleans, 2002.

A. Askenfelt and E.V. Jansson. From touch to string vibrations .1. timing in the grand piano action. *Journal of the Acoustical Society of America,* 88(l):52-63, 1990.

A. Askenfelt and E.V. Jansson. From touch to string vibrations .2. the motion of the key and hammer. *Journal of the Acoustical Society of America,* 90(5):2383^93, 1991.

AUDI. Mmi controller. URL: http://www.audi.com.

M. Badescu, C. Wampler, and C. Mavroidis. Rotary haptic knob for vehicular instrument controls. In *Proceedings of the Tenth Symposium on Haptic Interfaces for Virtual Environment and Teleoperator Systems.* Orlando, FL, March 2002.

BMW. idrive controller. URL: http://www.bmw.com.

C. Cadoz, L. Lisowski, and J. L. Florens. A modular feedback keyboard design. *Computer Music Journal,* 14 (2):47-51, 1990.

J. D. Carlson, D. M. Catanzarite, and K. A. StClair. Commercial magneto-rheological fluid devices. *International Journal of Modem Physics B,* 10(23-24):2857^2865, 1996.

E. Altenmuller D. Parlitz, T. Peschel. Assessment of dynamic finger forces in pianists: effects of training and expertise. *Journal of Biomechanics,* 31(11):1063^67, 1998.

Delphi. Hydrocarbon-based mr fluid mrf-132dg. Product Bulletin, 2005.

B. Gillespie. *Haptic Display of Systems with Changing Kinematic Constraints : The Virtual Piano Action.* PhD thesis, Stanford University, 1996.

M. R. Jolly, J. W. Bender, and J. D. Carlson. Properties and applications of commercial magnetorheological fluids. *Journal of Intelligent Material Systems and Structures,* 10(1):5-13, 1999.

LORD. *Permanent-Electromagnet Systems.* The Lord Corporation, Thomas Lord Research Center, Cary, NC (USA), 2002.

LORD. *Hydrocarbon-Based MR Fluid MRF132-DG Product Bulletin.* The Lord Corporation, Thomas Lord Research Center, Cary, NC (USA), 2005.

LORD. Designing with mr fluids. In *Lord Corporation Engineering note,* Thomas Lord Research Center, Cary, NC (USA), Dec. 1999.

J. Lozada, M. Hafez, and X. Boutillon. A novel haptic interface for musical keyboards. In *Advanced Intelligent Mechatronics.* Zurich, 2007.

D. Meisel. Key actuation systems for keyboard instruments, Nov. 2003.

J. Melli-Huber, B. Weinberg, A. Fisch, J. Nikitczuk, C. Mavroidis, and C. Wampler. Electro-rheological fluidic actuators for haptic, vehicular instrument controls. In *11th Symposium on Haptic Interfaces for Virtual Environment and Teleoperator Systems (HAPTICS'03).* Los Angeles, California, U.S.A, March 2003.

M. R. Reed and W. J. Book. Modeling and control of an improved dissipative passive haptic display. In *2004 Ieee International Conference on Robotics and Automation, Vols 1- 5, Proceedings,* Ieee International Conference on Robotics and Automation, pages 311-318. 2004.

B.H. Repp. Effects of auditory feedback deprivation on expressive piano performance. *Music Perception,* 16(4): 409-38, 1999.

Mechatronic Systems Applications

Edited by Annalisa Milella Donato Di Paola and Grazia Cicirelli

ISBN 978-953-307-040-7
Hard cover, 352 pages
Publisher InTech
Published online 01, March, 2010
Published in print edition March, 2010

Mechatronics, the synergistic blend of mechanics, electronics, and computer science, has evolved over the past twenty five years, leading to a novel stage of engineering design. By integrating the best design practices with the most advanced technologies, mechatronics aims at realizing high-quality products, guaranteeing at the same time a substantial reduction of time and costs of manufacturing. Mechatronic systems are manifold and range from machine components, motion generators, and power producing machines to more complex devices, such as robotic systems and transportation vehicles. With its twenty chapters, which collect contributions from many researchers worldwide, this book provides an excellent survey of recent work in the field of mechatronics with applications in various fields, like robotics, medical and assistive technology, human-machine interaction, unmanned vehicles, manufacturing, and education. We would like to thank all the authors who have invested a great deal of time to write such interesting chapters, which we are sure will be valuable to the readers. Chapters 1 to 6 deal with applications of mechatronics for the development of robotic systems. Medical and assistive technologies and human-machine interaction systems are the topic of chapters 7 to 13.Chapters 14 and 15 concern mechatronic systems for autonomous vehicles. Chapters 16-19 deal with mechatronics in manufacturing contexts. Chapter 20 concludes the book, describing a method for the installation of mechatronics education in schools.

How to reference

In order to correctly reference this scholarly work, feel free to copy and paste the following:

Jose Lozada, Samuel Roselier, Florian Periquet, Xavier Boutillon and Moustapha Hafez (2010). Magneto-Rheological Technology for Human-Machine Interaction, Mechatronic Systems Applications, Annalisa Milella Donato Di Paola and Grazia Cicirelli (Ed.), ISBN: 978-953-307-040-7, InTech, Available from: http://www.intechopen.com/books/mechatronic-systems-applications/magneto-rheological-technology-for-human-machine-interaction

INTECH
open science | open minds

InTech Europe
University Campus STeP Ri
Slavka Krautzeka 83/A
51000 Rijeka, Croatia
Phone: +385 (51) 770 447

InTech China
Unit 405, Office Block, Hotel Equatorial Shanghai
No.65, Yan An Road (West), Shanghai, 200040, China
中国上海市延安西路65号上海国际贵都大饭店办公楼405单元
Phone: +86-21-62489820

Fax: +385 (51) 686 166
www.intechopen.com

Fax: +86-21-62489821

IntechOpen